



Fluor-silane modified nano-calcium carbonate (CaCO_3) as a hydrophobic coating for the conservation of sandstone via bio-inspired design

Ye Wang, Wenxin Xiao, Danqian Wang, Jingfeng Wang*

College of Materials Science and Engineering, Chongqing University, Chongqing 400045, China



ARTICLE INFO

Keywords:

Red sandstone
 Nano CaCO_3
 Acid rain corrosion
 Hydrophobicity

ABSTRACT

Ancient cultural relics built of red sandstone have high historical value. However, due to the acceleration of the industrialization process of human civilization, increasingly frequent acid rain has caused irreversible damage to the surface of red sandstone artifacts. In this research, a fluor-silane modified nano-calcium carbonate (CaCO_3) was prepared as a biomimetic hydrophobic coating for the conservation of red sandstone inspired by the lotus leaf effect. Characterizations and immersion tests were carried out to assess the protective properties of the coating. XRD, FT-IR, TEM and SEM were combined to characterize the morphology of the coating. In addition, the water contact angle was measured before and after immersion in the simulated acid rain. The results indicate that this kind of hydrophobic nano- CaCO_3 coating effectively protected the sandstone from the deleterious effects of acid rain.

1. Introduction

As a natural mineral, red sandstone has been widely used in various buildings worldwide due to its beauty and ease of carving, which has made it an ideal choice for sculptural and decorative architectural elements (Amalia Yunia Rahmawati, 2020). However, red sandstone is relatively susceptible to erosion, so in some areas, after hundreds of years of weathering and erosion, it may experience wear and the loss of some details (Rodrigues, 2001). For example, due to acid rain caused by air pollution, the Leshan Giant Buddha has suffered significant corrosion, leading to severe damage to the cultural relic (Sun et al., 2021). Therefore, the preservation and restoration of stone cultural relics is of utmost urgency (Cappelletti et al., 2015; Wu et al., 2023).

Among all protective measures, developing surface hydrophobic coatings may be an effective approach. Inspired by the lotus leaf effect, various bionic hydrophobic coatings have been widely developed in recent years for surface protection of various materials (Kulinich & Farzaneh, 2009; Lu et al., 2015; Wu et al., 2019a). It has been well established that sufficient surface roughness and low surface energy substances are considered to be two important factors for surface hydrophobicity (Yeganeh & Mohammadi, 2018). However, the surface of red sandstone usually appears hydrophilic due to its high surface energy (Ali et al., 2020). Therefore, it seems feasible to further increase its surface roughness through nanoparticles and use some surface energy

substances to reduce the surface energy of red sandstone to achieve hydrophobicity. According to previous researches, many nano particles (CaCO_3 (Wang et al., 2020), SiO_2 (Wang et al., 2023a), TiO_2 (Munafò et al., 2015), etc.) have been investigated to develop hydrophobic coatings used for the preservation of building materials. In addition, silanes (Wu et al., 2019b), stearic acid (Ng et al., 2010), and lauric acid (Wu et al., 2021), etc. have also been revealed to be effective in reducing the surface energy. For example, Wang et al. (2023a) prepared a kind of nanocomposite coating of silica for the sandstone protection. They found that the rough structure can be formed by the SiO_2 particles. Then, the isobutyltriethoxysilane (IBTES) with hydrophobic groups was added to lower the surface energy to achieve water repellency.

Calcium carbonate (CaCO_3) has been widely used in the engineering field due to its low cost (Wang et al., 2023c; Zaliman et al., 2022). The novel microbial induced calcite precipitation (MICP) has been directly used to consolidate calcareous sands recently (Chen et al., 2023; Kou et al., 2023), which demonstrated high engineering application value. Moreover, calcareous sand reinforced with CaCO_3 can even have better durability in harsh marine environments (Li et al., 2023b). In our previous research, CaCO_3 was used as protective coatings on the surface of bare Mg alloy (Wang et al., 2023f) and PEO coatings (Wang et al., 2023g). The results demonstrated that the CaCO_3 layer significantly enhanced the anticorrosion property of Mg alloys. Moreover, self-

* Corresponding author.

E-mail address: jfwang@cqu.edu.cn (J. Wang).

healing performance could also be observed in the environment of Cl⁻-containing PC paste. Besides, our previous study (Wang et al., 2023e) successfully developed a super-hydrophobic durian-peel like CaCO₃ coating on the surface of Mg alloy by the novel ultrasound-assisted chemical conversion method to enhance its corrosion resistance against chloride ions. It was demonstrated that the hydrophobic CaCO₃ coating can greatly improve the corrosion resistance of the substrate. Additionally, CaCO₃ powder coatings have also been widely studied due to their environmental and economic advantages. Yu et al. (Yu et al., 2006) developed a nano-CaCO₃ modified epoxy powder coating. They found that the tensile property, cupping property and neutral salt spray corrosion resistance of the coating were significantly enhanced after the modification.

This study aims to develop a new kind of hydrophobic nano CaCO₃ coating for the conservation of sandstone cultural relics exposed to outdoor environments. Isopropanol ethanol and anhydrous ethanol were used to achieve a better dispersion of nano CaCO₃ particles. Therefore, the nano CaCO₃ particles can act as nano-protrusions similar to those on lotus leaves.

Meanwhile, fluor-silane was also added to reduce the surface energy to achieve the hydrophobic property. Afterwards, the bionic hydrophobic coating could be achieved. Then, surface characterizations were carried out to obtain the morphology and waterproofing performance of the CaCO₃ coating. In addition, water contact angles of the specimens without and with the coating were also measured. Finally, an immersion test in an artificial acid rain solution was carried out to evaluate the durability of this coating. This kind of low-cost and efficient preparation of hydrophobic nano CaCO₃ coating that can be applied over a wide area provides practical value for the protection of cultural relics.

2. Experimental

2.1. Raw materials

The sandstone used in this research is the red sandstone, which does not contain clay. Then, specimens with the size of $\Phi 20 \times 10 \text{ mm}^3$ were prepared for use. Nanometer CaCO₃ particles and 1H, 1H, 2H, 2H-Perfluorodecyl-triethoxy silane ($\text{C}_{13}\text{H}_{13}\text{F}_{17}\text{O}_3\text{Si}$) were purchased from Shanghai Macklin Biochemical Co. Ltd., China, and the size of the CaCO₃ particles is about 50 nm. Isopropanol ethanol ($\text{C}_3\text{H}_8\text{O}$) was purchased from Chengdu Kelong Chemical Reagent Co. Ltd., China. Anhydrous ethanol ($\text{CH}_3\text{CH}_2\text{OH}$) was purchased from Chongqing Chuandong Chemical Reagent Co. Ltd., China. The artificial acid rain solution was made by mixing the sulfuric acid, nitrates with deionized water and the pH was adjusted to 2.3 to simulate the strong acid rain.

2.2. Preparation of the coating

Firstly, 5 g of isopropanol ethanol and 5 g of anhydrous ethanol were mixed. Then, 0.1 g nano CaCO₃ particles were dispersed in the solution. Afterwards, 2 g of 1H, 1H, 2H, 2H-Perfluorodecyl-triethoxy silane was added into the solution. Then, the mixture was stirring at 25 °C for 2 h. The schematic diagram of the preparation process is shown in Fig. 1a.

The protective CaCO₃ coating was then brushed on the sandstones for three times, with an interval of ten minutes each time.

2.3. Characterization of the coating

The crystal structure of the CaCO₃ powder was analyzed by X-ray diffraction (XRD, PANalytical X'Pert Powder, Netherlands) using Cu-K_α radiation operated with a scanning range set between 5° and 90° at 60 kV and 55 mA. The chemical bonds existing in the CaCO₃ powder were confirmed using a Fourier transform infrared spectrophotometer (FT-IR, Nicolet 380, Thermo Electron Corporation, USA). The morphology of the CaCO₃ particles was examined by the transmission

electron microscopy (TEM, Thermo Fisher Scientific Talos F200S, Czech Republic). The surface morphology and corresponding elemental mapping analyses of the sandstone without and with the coating were examined by the scanning electron microscopy (SEM, ZEISS Sigma 300, Germany). The water contact angles (WCA) of the obtained coatings were measured using a drop-shape analysis system (Dataphysics OCA20, China).

2.4. Immersion test

The immersion test was carried out in a strong artificial acid rain solution (pH = 2.3). Except for the surface painted with the hydrophobic nano CaCO₃ coating, all other surfaces of the sample were sealed with the epoxy resin. The sample without coating was also immersed as a comparison sample with only one surface exposed. The immersion experiment was continued for 7 days at room temperature (25 °C ± 2 °C).

3. Results and discussion

3.1. Characterization of the nano CaCO₃ particles

Fig. 1(b-c) shows the X-ray powder diffraction (XRD) pattern and the FT-IR spectrum of the nano CaCO₃ powder. From the XRD pattern in Fig. 1b, it can be identified that the phase composition of the nano CaCO₃ powder is calcite (PDF: 99-0022). It is known that calcium carbonate usually has three anhydrous crystalline phases: calcite, vaterite and aragonite (Du & Amstad, 2020). The solubility product constants (K_{sp}) for these phases are 3.36×10^{-9} , 4.6×10^{-9} , and 1.2×10^{-8} . These values suggest that calcite is thermodynamically more stable than aragonite and vaterite (Jamesh et al., 2011). It has been reported that calcite has good chemical stability and unique particle structure, which can provide good filling and hiding power, and can also improve the wear resistance of the coating (Wu et al., 2016). Moreover, calcite has also been used in civil engineering recently to repair the cracked soil (Roksana et al., 2023). This kind of cubic-shaped particles can also effectively increase the surface roughness of red sandstone, which is essential for the formation of a hydrophobic surface (Wang et al., 2023e).

In addition, the characterization of CaCO₃ nano particles by FT-IR in Fig. 1c shows the absorption band around 1390 cm^{-1} , which can be identified as the C=O bond. Furthermore, the peaks observed at 870 cm^{-1} and 711 cm^{-1} can be attributed to the intramolecular vibrations of CO₃²⁻ groups (Kang et al., 2018).

Fig. 1(d-g) presents the TEM morphology of the CaCO₃ particles and the corresponding EDS analysis results. It can be observed in Fig. 1d that the CaCO₃ particles are in a cubic shape, which is the typical shape of calcite (Wang et al., 2023d). Previous studies have reported that vaterite is usually ellipsoidal, whereas aragonite is often needle-shaped crystal (Chen et al., 2006; Wang et al., 2023b). Additionally, the diameter of these particles is approximately 50 nanometers, underscoring the nanoscale nature of the CaCO₃ powder. Previous literature has shown that when the surface energy of such cubic particles was reduced by using some low surface energy substances, a hydrophobic surface can be obtained (Wang et al., 2020). At the same time, the self-cleaning property can also be achieved. In addition, the EDS analysis results in Fig. 1(e-g) also reveal that the compositional elements of these particles are Ca, O and C.

3.2. Surface morphology of the hydrophobic nano CaCO₃ coating

Fig. 2 illustrates the surface characteristics of red sandstone alongside the corresponding Energy Dispersive Spectroscopy (EDS) analyses pre- and post-application of the hydrophobic nano CaCO₃ coating. In Fig. 2a and b, the surface morphology of the sandstone primarily consists of particles larger than 2 μm. It has been reported that red sandstone was predominantly constituted of quartz (SiO₂), which imparted

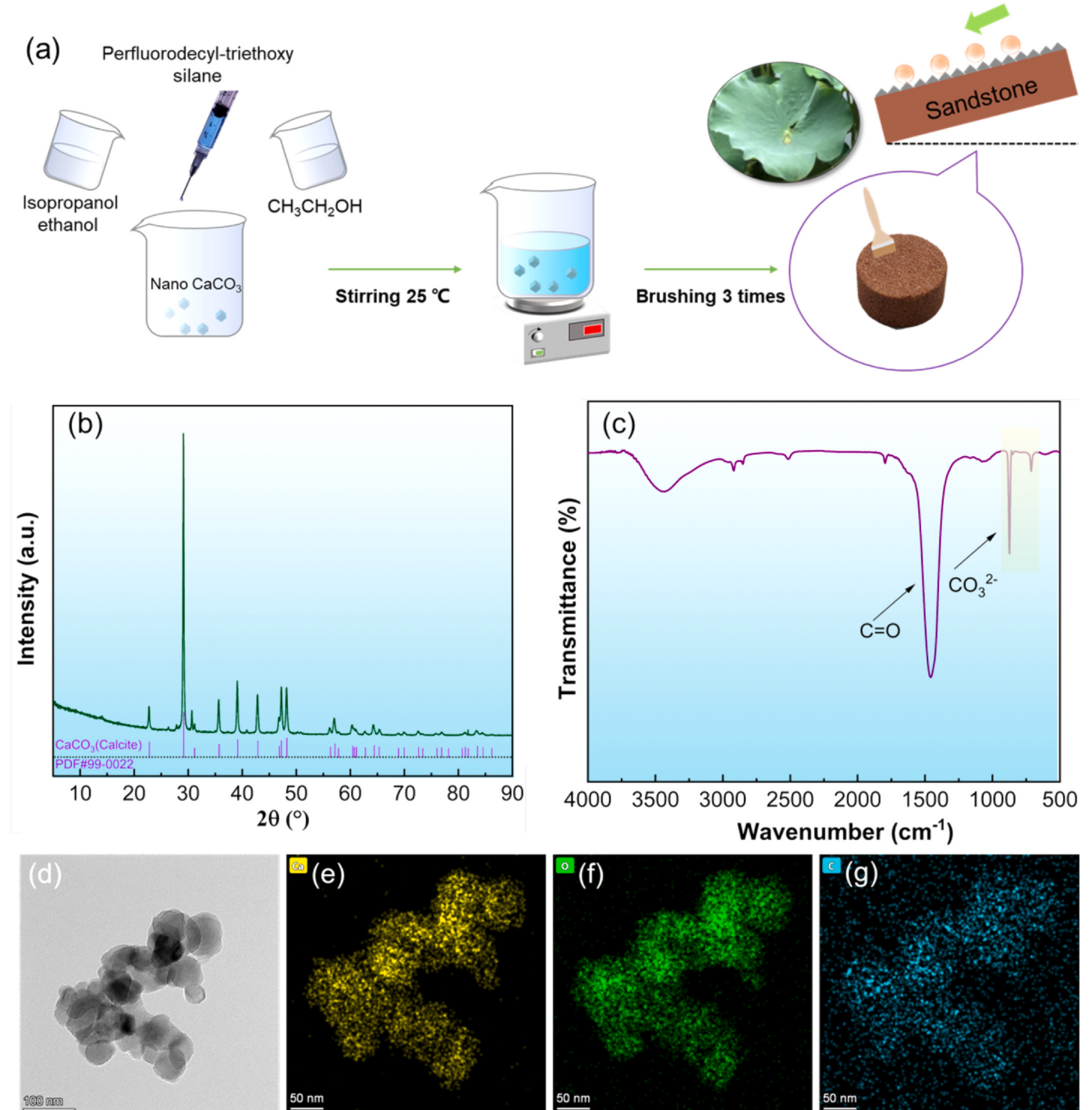


Fig. 1. (a) Schematic diagram of the preparation process of the bionic hydrophobic nano CaCO_3 coating; (b) XRD pattern; (c) FT-IR spectrum of the nano CaCO_3 powder; (d) TEM image of CaCO_3 nanoparticles; (e-g) corresponding EDS analysis results.

mechanical robustness to its structure (Li et al., 2023a). Additionally, trace amounts of Al_2O_3 and Fe_2O_3 were known to be present based on prior literature (Potysz & Bartz, 2023). Furthermore, Fig. 2(b1-b6) present the elemental mapping results corresponding to Fig. 2b. These mappings reveal that the sandstone is predominantly composed of Si and O elements, accompanied by minimal traces of C, Ca, and Fe elements, which is in good agreement with the previous researches.

In comparison, when the surface was coated with the nano CaCO_3 coating, the surface morphology of the sandstone became quite different. It can be seen from Fig. 2c and d that, apart from the initial micron-sized particles, nano-sized particles have been adhered to the surface. This

reveals that nano CaCO_3 particles have been coated on the surface of the sandstone, which could be beneficial for the rough structure that the hydrophobic surface needs. Furthermore, as can be seen from the mapping results in Fig. 2(d1-d6), the surface contains more Ca and C elements but less Si element, which also demonstrates the attachment of the nano CaCO_3 particles on the original surface. As a comparison with Fig. 2(b6), in Fig. 2(d6), the emergence of the F element is notably apparent, which is attributed to the incorporation of fluor silane. This reveals that the surface of the sandstone has been uniformly covered by the hydrophobic nano CaCO_3 coating. The wetting performance and self-cleaning property of the hydrophobic CaCO_3 coating are measured in the next section.

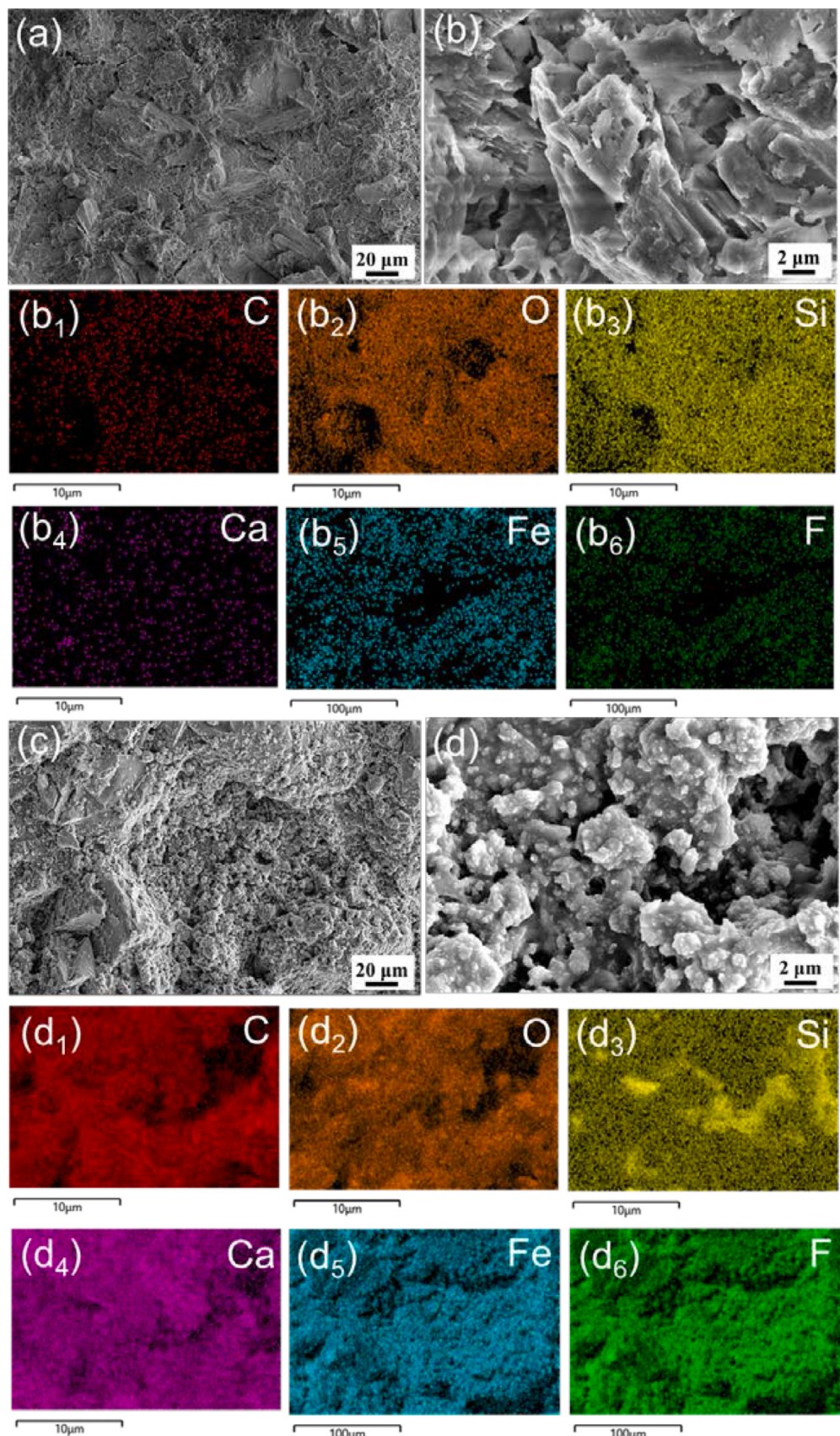


Fig. 2. SEM images of the sandstone (a, b) before and (c, d) after brushing the nano CaCO_3 coating, (b₁-b₆) and (d₁-d₆) shows the EDS analysis results of (b) and (d).

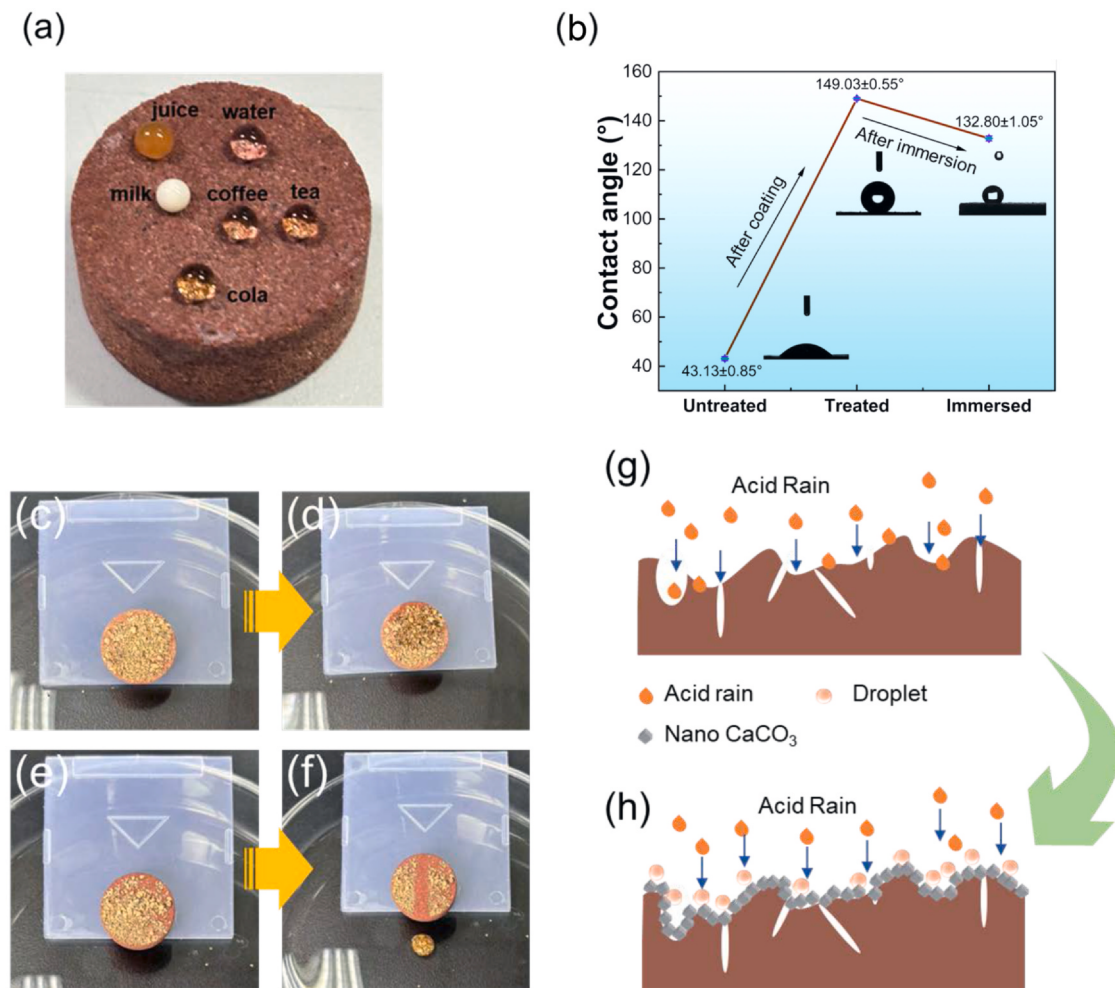


Fig. 3. (a) Comparisons of a variety of different liquids poured on the surface of a sandstone sample coated with the hydrophobic nano CaCO₃ coating; (b) Evolution of the water contact angles of the sandstone and after the coating process, as well as after immersion in the simulated acid rain for 7 days, the insets in (b) depict the morphology of water droplets; (c-f) Self-cleaning ability of the investigated samples: (c, d) Untreated specimen, (e, f) Treated specimen; (g, h) Protection mechanism of the hydrophobic nano CaCO₃ coating against acid rain.

3.3. Wetting performance and self-cleaning property of the hydrophobic nano CaCO₃ coating

Fig. 3(a-b) shows the water contact angles of the sandstone before and after brushing the hydrophobic nano CaCO₃ coating. In addition, after immersion in the artificial acid rain for 7 days, the contact angle of the coated specimen was also measured. It can be seen from Fig. 3a that the surface of the sandstone after the application of the hydrophobic nano CaCO₃ coating exhibits an excellent repellent performance against different liquids. When in contact with juice, milk, tea, coffee and cola, intact droplets can still exist on the surface of the sandstone. This indicates that this kind of hydrophobic coating can deal with the erosion of red sandstone by a variety of liquids. For better quantitative analysis, the water contact angles of the specimens were measured and the results are presented in Fig. 3b. It can be seen that the water contact angle of the bare sandstone surface is $43.13^\circ \pm 0.85^\circ$, which demonstrates the hydrophilic property. Meanwhile, when the sandstone is coated with the CaCO₃ coating, the contact angle of the specimen increases to $149.03^\circ \pm 0.55^\circ$. It is well known that when the contact angle of the surface is higher than 90° , it presents a hydrophobic property. Moreover, when the contact angle is greater than 150° , a superhydrophobic surface can be obtained which often possesses the excellent self-cleaning performance (Kulinich & Farzaneh, 2009). Therefore, due to the contact angle of the sandstone with the CaCO₃ coating is much

higher than 90° and is close to 150° , this reveals that the surface has an excellent hydrophobic property and the self-cleaning property will be measured in the next section.

In addition, after being immersed in the strong artificial acid rain for 7 days, water contact angle of the coated specimen was also measured. As shown in Fig. 3b, the contact angle of the coated specimen can still reach $132.80^\circ \pm 1.05^\circ$. This means that even though the acid rain is highly corrosive, the surface coating can be well preserved after a relatively long-term immersion, which can provide enough corrosion resistance for the red sandstone.

Fig. 3(c-f) exhibits the results of the self-cleaning ability of the untreated and treated specimens.

As can be seen from Fig. 3c and d, the water droplet penetrates directly into the sand grains due to the hydrophilic nature of the sandstone surface. This indicates that if the surface of the sandstone left untreated, the surface of the sandstone will come into direct contact with acid rain solutions, which is the primary reason for the corrosion of the sandstone surface. In contrast, after applying the hydrophobic nano CaCO₃ coating (Fig. 3e and f), the water droplet carries the grits on the surface and rolls down directly, keeping the surface dry and clean. Therefore, it indicates that the treated specimen has an exclusive self-cleaning effect compared to the untreated one, which is crucial for the red sandstone to remain well preserved in outdoor environments.

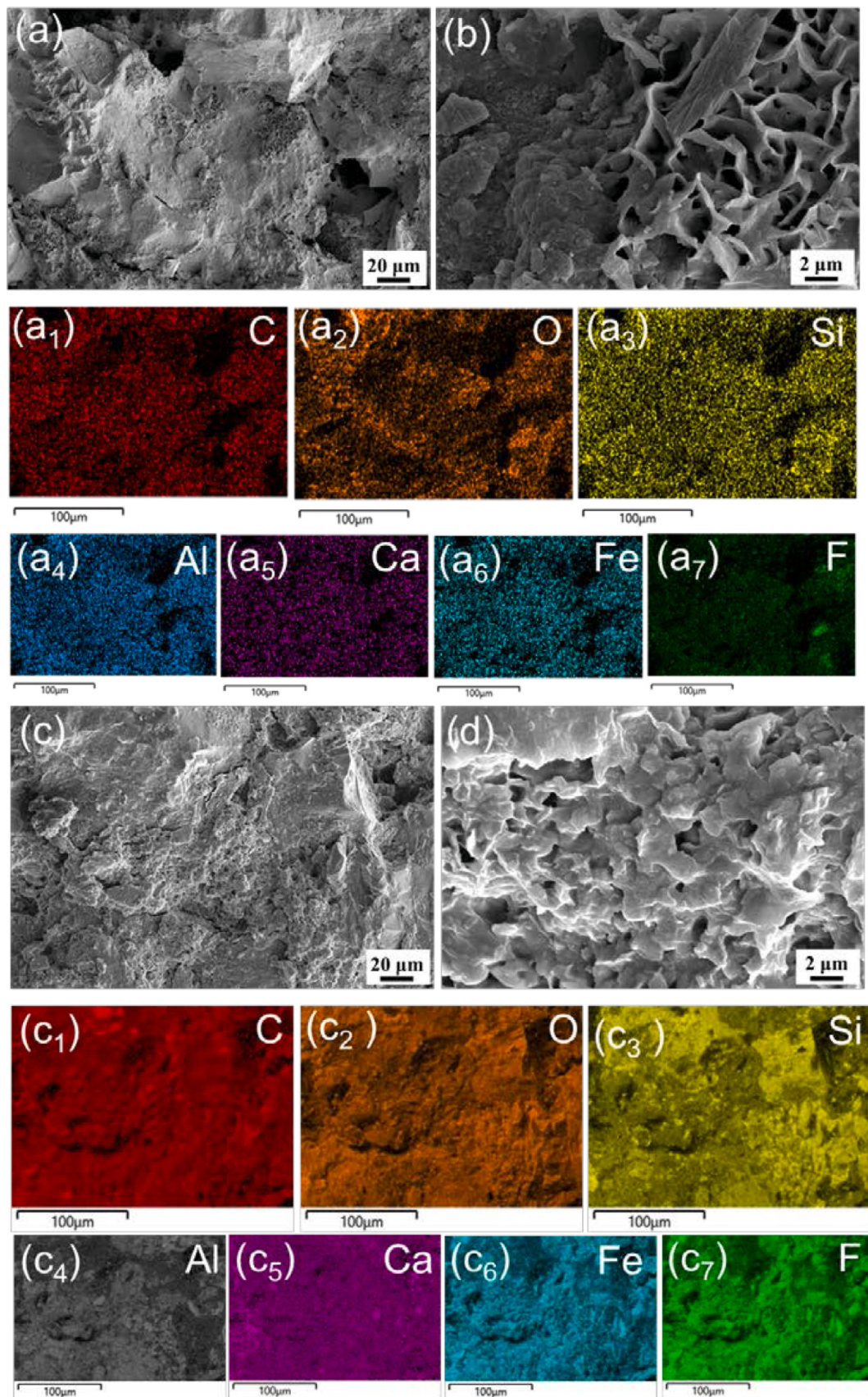


Fig. 4. SEM images of the sandstone (a, b) before and (c, d) after brushing the hydrophobic nano CaCO_3 coating after immersion in the simulated acid rain solution for 7 days, (a₁-a₇) and (c₁-c₇) shows the EDS analysis results corresponding to (a) and (c).

3.4. Surface morphology of the hydrophobic nano CaCO_3 coating after immersion

In order to better evaluate the durability of this hydrophobic nano CaCO_3 coating in acid rain, an immersion test in the strong artificial acid rain solution was carried out on both untreated and treated specimens up to 7 days. Then the surface morphologies of both specimens are shown in Fig. 4. It can be noted from Fig. 4a that large particles are still visible in the sandstone after immersion. In addition, a sheet-like structure can be observed on the surface, which is different from that before the immersion. This could be related to the generation of some corrosion products due to the reactions between sandstone and the acid rain solution. Moreover, the EDS results in Fig. 4(a1-a7) show that the surface consists mainly of Si, Al, Ca and Fe elements but little C and O elements, which is similar to that before the immersion test. However, combined with the SEM images and EDS results, it is concluded that corrosion has occurred during the immersion period. As a comparison, the surface morphology of the sandstone with the hydrophobic nano CaCO_3 coating after immersion is shown in Fig. 4c and d. It can be noted that the surface morphology of this specimen was similar to that before immersion, whereas it was completely different to that without the coating. Fig. 4c shows that the structure of the sandstone was well preserved due to the protection of the CaCO_3 coating. Moreover, the enlarged image in Fig. 4d reveals that although some of the nano CaCO_3 particles were dissolved in the acid rain solution, but a lot of nanoparticles were still preserved. This indicates that the hydrophobic nano CaCO_3 coating can still protect the surface of the sandstone after the long-term immersion in the strong acid rain solution. Furthermore, according to the EDS analysis results in Fig. 4(c1-c7), apart from the elements C, O, Si, Al, Ca and Fe elements, the F element can still be detected over the surface, which comes from the fluor silane. It reveals that the coating still has an excellent coverage on the surface after the immersion. Additionally, compared to Fig. 4(a5) more Ca and C elements can be detected in Fig. 4(c1) and (c5), which also demonstrates the protective property of the nano CaCO_3 coating.

3.5. Protection mechanism of the hydrophobic nano CaCO_3 coating

As mentioned above, a hydrophobic CaCO_3 coating was prepared by the modification of silane on nano CaCO_3 particles. It has been reported that the red sandstone mainly consists of SiO_2 , Al_2O_3 and Fe_2O_3 , etc. (Potysz & Bartz, 2023), which can easily react with the acid rain, the detailed reactions are as follows:



If the surface of sandstone is in direct contact with acid rain for a long period of time, corrosion can occur and cause severe damage to the sandstone. When applying a coating on the surface of red sandstone artifacts, it will effectively prevent direct exposure to acid rain. Furthermore, if the hydrophobic surface can be achieved, it has the potential to bring about a substantial shift in the situation.

Previous research predominantly attributed the exceptional hydrophobic properties of coatings to the Wenzel model (Han et al., 2007) and the Cassie model (Wang et al., 2011), respectively. Typically, air pockets entrapped between the nano particles serve as a protective barrier, shielding the substrate from corrosion (Wu et al., 2019b). Among the coating, structured surfaces facilitate the formation of air pockets. In the case of a hierarchical structure, air pockets within the grooves beneath the liquid diminish the contact area between the liquid and the surface, leading to a reduction in contact angle and adhesive force. Therefore, the hydrophobic nano CaCO_3 coating developed in this study can also be elucidated through the Cassie model, with the

water contact angle (WCA) being determinable using the Cassie-Baxter equation:

$$\cos \theta_r = f_1 \cos \theta - f_2 \quad (4)$$

In Eq. (4), the variables f_1 and f_2 denote the contact area ratios for water- CaCO_3 and air-water interfaces, respectively. Meanwhile, θ_r and θ represent the contact angles for the treated samples and the bare red sandstone, respectively. As $f_1 + f_2 = 1$, the equation can be expressed as:

$$\cos \theta_r = f_1 (\cos \theta + 1) - 1 \quad (5)$$

As the CA of the bare red sandstone is about 43.13° , the CA of the treated specimen is 149.03° , so the f_1 value for the hydrophobic surface is around 8.24 %, thus the f_2 value is 91.76 %, which is a large fraction of the air at the interface and thus prevents the permeation of the corrosion ions and enhances the corrosion resistant performance. The detailed protection mechanism is shown in Fig. 3(g-h).

4. Conclusions

In this study, fluor silane-modified nano CaCO_3 particles were employed as a bionic hydrophobic coating to conserve the red sandstone. The immersion test up to 7 days was adopted in the strong artificial acid rain to assess the corrosion resistance of the as-prepared hydrophobic nano CaCO_3 coating. Meanwhile, XRD, FT-IR were carried out to determine the phase composition of the CaCO_3 was calcite. In addition, SEM observation confirmed the attachment of the coating to the surface. Based on the results obtained, the main conclusions can be drawn as follows:

1. A comparison with bare sandstone revealed that nano-sized CaCO_3 particles adhered to the surface of the coated sandstone after the application of the hydrophobic coating.
2. The water contact angle increased from $43.13 \pm 0.85^\circ$ to $149.03 \pm 0.55^\circ$ after applying this hydrophobic nano CaCO_3 coating. Moreover, a self-cleaning performance can also be achieved. In addition, after immersion in the strong artificial acid rain for 7 days, the water contact angle remained at $132.80 \pm 1.05^\circ$.
3. After the immersion test, the surface of the coated sandstone was preserved well. Consequently, this nano CaCO_3 coating presents itself as a promising candidate for safeguarding sandstone against the corrosive effects of acid rain.

CRediT authorship contribution statement

Ye Wang: Writing – original draft, Methodology, Investigation, Conceptualization. **Wenxin Xiao:** Investigation. **Danqian Wang:** Visualization, Supervision. **Jingfeng Wang:** Supervision, Conceptualization.

Declaration of Competing Interest

The authors declare that they have no known competing financial interests or personal relationships that could have appeared to influence the work reported in this paper.

Acknowledgements

The authors gratefully acknowledge the financial support from the National Key Research and Development Program of China (No. 2021YFB3701100), the Natural Science Foundation Commission of China (Grant No. U20A20234 and 51874062), Chongqing Foundation and Advanced Research Project (Grant No. cstc2019jcyj-zdxmX0010), the Science and Technology Major Project of Shanxi Province (No. 20191102008).

References

- Ali, A. M., Yahya, N., & Qureshi, S. (2020). Interactions of ferro-nanoparticles (hematite and magnetite) with reservoir sandstone: implications for surface adsorption and interfacial tension reduction. *Petroleum Science*, 17(4), 1037–1055. <https://doi.org/10.1007/s12182-019-00409-w>
- Amalia Yunia Rahmawati. (2020). Geosciences in Archaeometry Methods and Case Studies.
- Cappelletti, G., Fermo, P., & Camiloni, M. (2015). Smart hybrid coatings for natural stones conservation. *Progress in Organic Coatings*, 78, 511–516. <https://doi.org/10.1016/j.porgcoat.2014.05.029>
- Chen, S. F., Yu, S. H., Hang, J., Li, F., & Liu, Y. (2006). Polymorph discrimination of CaCO₃ mineral in an ethanol/water solution: Formation of complex vaterite superstructures and aragonite rods. *Chemistry of Materials*, 18(1), 115–122. <https://doi.org/10.1021/cm0519028>
- Chen, Y., Han, Y., Zhang, X., Sarajpoor, S., Zhang, S., & Yao, X. (2023). Experimental study on permeability and strength characteristics of MICP-treated calcareous sand. *Biogeotechnics*, 1(3), Article 100034. <https://doi.org/10.1016/j.bgttech.2023.100034>
- Du, H., & Amstad, E. (2020). Water: How does it influence the CaCO₃ dormation? *Angewandte Chemie - International Edition*, 59(5), 1798–1816. <https://doi.org/10.1002/anie.201903662>
- Han, T. Y., Shr, J. F., Wu, C. F., & Hsieh, C. Te (2007). A modified Wenzel model for hydrophobic behavior of nanostructured surfaces. *Thin Solid Films*, 515(11), 4666–4669. <https://doi.org/10.1016/j.tsf.2006.11.008>
- Jamesh, M., Kumar, S., & Sankara Narayanan, T. S. N. (2011). Corrosion behavior of commercially pure Mg and ZM21 Mg alloy in Ringer's solution - Long term evaluation by EIS. *Corrosion Science*, 53(2), 645–654. <https://doi.org/10.1016/j.corsci.2010.10.011>
- Kang, Z., Zhang, J., & Niu, L. (2018). A one-step hydrothermal process to fabricate superhydrophobic hydroxyapatite coatings and determination of their properties. *Surface and Coatings Technology*, 334(November 2017), 84–89. <https://doi.org/10.1016/j.surcoat.2017.11.007>
- Kou, H., He, X., Li, Z., Fang, W., Zhang, X., An, Z., & Wu, Y. (2023). Biogeotechnics Effect of drying-wetting cycles on the durability of calcareous sand reinforced by MICP and recycled shredded coconut coir (RSC). *Biogeotechnics* Article 100038. <https://doi.org/10.1016/j.bgttech.2023.100038>
- Kulinich, S. A., & Farzaneh, M. (2009). Effect of contact angle hysteresis on water droplet evaporation from super-hydrophobic surfaces. *Applied Surface Science*, 255(7), 4056–4060. <https://doi.org/10.1016/j.apsusc.2008.10.109>
- Li, S., Huang, M., Cui, M., Xu, K., & Jin, G. (2023a). Thermal and mechanical properties of bio-cemented quartz sand mixed with steel slag. *Biogeotechnics*, 1(3), Article 100036. <https://doi.org/10.1016/j.bgttech.2023.100036>
- Li, Y., Li, Y., Guo, Z., & Xu, Q. (2023b). Durability of MICP-reinforced calcareous sand in marine environments: Laboratory and field experimental study. *Biogeotechnics*, 1(2), Article 100018. <https://doi.org/10.1016/j.bgttech.2023.100018>
- Lu, Z., Wang, P., & Zhang, D. (2015). Super-hydrophobic film fabricated on aluminium surface as a barrier to atmospheric corrosion in a marine environment. *Corrosion Science*, 91, 287–296. <https://doi.org/10.1016/j.corsci.2014.11.029>
- Munafò, P., Goffredo, G. B., & Quagliarini, E. (2015). TiO₂-based nanocoatings for preserving architectural stone surfaces: An overview. *Construction and Building Materials*, 84, 201–218. <https://doi.org/10.1016/j.conbuildmat.2015.02.083>
- Ng, W. F., Wong, M. H., & Cheng, F. T. (2010). Stearic acid coating on magnesium for enhancing corrosion resistance in Hanks' solution. *Surface and Coatings Technology*, 204(11), 1823–1830. <https://doi.org/10.1016/j.surcoat.2009.11.024>
- Potysz, A., & Bartz, W. (2023). Dissolution of red sandstones exposed to siderophore-producing bacterium Pseudomonas fluorescens: Experimental biowathering coupled to a geochemical model. *Construction and Building Materials*, 369, Article 130584. <https://doi.org/10.1016/j.conbuildmat.2023.130584>
- Rodrigues, J. D. (2001). Consolidation of decayed stones. A delicate problem with few practical solutions. *Historical Constructions*, 3–14.
- Roksana, K., Aluthgun, S., Montalbo, M., & Tang, C. (2023). Biogeotechnics Desiccation cracking remediation through enzyme induced calcite precipitation in fine-grained soils under wetting drying cycles. *Biogeotechnics* Article 100049. <https://doi.org/10.1016/j.bgttech.2023.100049>
- Sun, B., Zhang, P., Shen, X., & Liu, Y. (2021). Characterizing-water seepage damage in the chest-abdomen area of the Leshan Giant Buddha. *Japanese Geotechnical Society Special Publication*, 9(8), 403–411. <https://doi.org/10.3208/jgssp.v09.cpeg087>
- Wang, G., Chai, Y., Li, Y., Luo, H., Zhang, B., & Zhu, J. (2023a). Sandstone protection by using nanocomposite coating of silica. *Applied Surface Science*, 615(2022), Article 156193. <https://doi.org/10.1016/j.apsusc.2022.156193>
- Wang, G. G., Zhu, L. Q., Liu, H. C., & Li, W. P. (2011). Self-assembled biomimetic superhydrophobic CaCO₃ coating inspired from fouling mineralization in geothermal water. *Langmuir*, 27(20), 12275–12279. <https://doi.org/10.1021/la202613r>
- Wang, M., Tan, X., Tu, Y., Xiang, P., Jiang, L., Yang, A., Xu, R., & Chen, X. (2020). Self-healing PDMS/SiO₂/CaCO₃ composite coating for highly efficient protection of building materials. *Materials Letters*, 265, Article 127290. <https://doi.org/10.1016/j.matlet.2019.127290>
- Wang, Y., Xiao, W., Ma, K., Dai, C., Wang, D., & Wang, J. (2023b). Enhancing corrosion resistance of the CaCO₃/MgO coating via ultrasound-assisted chemical conversion with addition of ethylenediamine tetra-acetic acid (EDTA) on AZ41 Mg alloy. *Surface and Coatings Technology*, 467, Article 129687. <https://doi.org/10.1016/j.surcoat.2023.129687>
- Wang, Y., Xiao, W., Ma, K., Dai, C., Wang, D., & Wang, J. (2023c). In-situ growth and anticorrosion mechanism of a bilayer CaCO₃ / MgO coating via rapid electrochemical deposition on AZ41 Mg alloy concrete formwork. *Journal of Materials Research and Technology*, 25, 6628–6643. <https://doi.org/10.1016/j.jmrt.2023.07.110>
- Wang, Y., Xiao, W., Ma, K., Dai, C., Wang, D., & Wang, J. (2023d). Towards development of anticorrosive CaCO₃ -coated passive layer on Mg alloy with ultrasound-assisted electrodeposition. *Corrosion Science*, 224, Article 111546. <https://doi.org/10.1016/j.corsci.2023.111546>
- Wang, Y., You, Z., Ma, K., Dai, C., Wang, D., & Wang, J. (2023e). Corrosion resistance of a superhydrophobic calcium carbonate coating on magnesium alloy by ultrasonic cavitation-assisted chemical conversion. *Corrosion Science*, 211. <https://doi.org/10.1016/j.corsci.2022.110841>
- Wang, Y., You, Z., Sanlve, P., Ma, K., Dai, C., Wang, D., ... Pan, F. (2023f). Corrosion resistance of a calcium carbonate coating prepared by ultrasound-assisted chemical conversion in calcium disodium edetate solution. *Journal of Magnesium and Alloys*. <https://doi.org/10.1016/j.jma.2022.11.022>
- Wang, Y., Yu, D., Ma, K., Dai, C., Wang, D., & Wang, J. (2023g). Self-healing performance and corrosion resistance of a bilayer calcium carbonate coating on microarc-oxidized magnesium alloy. *Corrosion Science*, 212, Article 110927. <https://doi.org/10.1016/j.corsci.2022.110927>
- Wu, F., Gao, S., Zeng, Y., Li, Y., Zhao, Z., & Shen, C. (2021). Study on synthesis and demolding performance of polyethylene glycol fatty acid mold release agents. *Polymers for Advanced Technologies*, 32(10), 4061–4069. <https://doi.org/10.1002/pat.5412>
- Wu, H., Shi, J., Xiao, Y., He, J., & Chu, J. (2023). Microbial mineralization: A promising approach for stone cultural relics restoration. *Biogeotechnics* Article 100053. <https://doi.org/10.1016/j.bgttech.2023.100053>
- Wu, W., Zhang, F., Li, Y. C., Zhou, Y. F., Yao, Q. S., Song, L., ... Chen, D. C. (2019b). Corrosion resistance of a silane/ceria modified Mg-Al-layered double hydroxide on AA5005 aluminum alloy. *Frontiers of Materials Science*, 13(4), 420–430. <https://doi.org/10.1007/s11706-019-0476-x>
- Wu, W. S., Queiroz, M. E., & Mohallem, N. D. S. (2016). The effect of precipitated calcium carbonate nanoparticles in coatings. *Journal of Coatings Technology and Research*, 13, 277–286.
- Yeganeh, M., & Mohammadi, N. (2018). Superhydrophobic surface of Mg alloys: A review. *Journal of Magnesium and Alloys*, 6(1), 59–70. <https://doi.org/10.1016/j.jma.2018.02.001>
- Yu, H. J., Wang, L., Shi, Q., Jiang, G. H., Zhao, Z. R., & Dong, X. C. (2006). Study on nano-CaCO₃ modified epoxy powder coatings. *Progress in Organic Coatings*, 55(3), 296–300. <https://doi.org/10.1016/j.porgcoat.2006.01.007>
- Zaliman, S. Q., Zakaria, N. A., Ahmad, A. L., & Leo, C. P. (2022). 3D-imprinted superhydrophobic polyvinylidene fluoride membrane contactor incorporated with CaCO₃ nanoparticles for carbon capture. *Separation and Purification Technology*, 287. <https://doi.org/10.1016/j.seppur.2022.120519>